On the transformation pathways of α-PbO$_2$-type TiO$_2$ at the twin boundary of rutile bicrystals and the origin of rutile bicrystals

Pouyan SHEN[1]*, Shyh-Lung HWANG[2], Hao-Tsu CHU[3], Tzen-Fu YUI[4], Chiennan PAN[1] and Wuu-Liang HUANG[5]

[1] Institute of Materials Science and Engineering, National Sun Yat-sen University, Kaohsiung, Taiwan, ROC
*Corresponding author, e-mail: pshen@mail.nsysu.edu.tw
[2] Department of Materials Science and Engineering, National Dong Hwa University, Hualien, Taiwan, ROC
[3] Central Geological Survey, P.O. Box 968, Taipei, Taiwan, ROC
[4] Institute of Earth Sciences, Academia Sinica, Taipei, Taiwan, ROC
[5] Department of Geosciences, National Taiwan University, Taipei, Taiwan, ROC

Abstract: Extraction and electron irradiation (under transmission electron microscopy) of an epitaxial nanometer-thick α-PbO$_2$-type TiO$_2$ slab between twinned rutile bicrystals in ultra-high pressure metamorphic rock caused phase changes into a modified fluorite-type and then an amorphous phase. This martensitic-type transition process accounts for the dislocations and stacking faults of the slab and disordering of Ti in the adjoined rutile bicrystals. Additional hydrothermal experiments of sol-gel TiO$_2$-Al$_2$O$_3$ performed at 8.5–9 kbar and 675–800°C in the piston-cylinder apparatus indicated that twinned rutile bicrystals were shaped in mirror image without the formation of α-PbO$_2$-type TiO$_2$ slab at the twin boundary and with no other planar defects for the bicrystals. The twinned bicrystals can be rationalized by growth and/or coalescence processes. Accordingly, it is not justified to assume a precursor phase of α-PbO$_2$-type structure for twinned rutile bicrystals when there is no such relic. Rutile, unless exsolved epitaxially from a host mineral such as garnet, does not constitute evidence for unusually deep burial for ultra-high pressure terranes.

Key-words: α-PbO$_2$-type TiO$_2$, transformation path, twinned rutile, ultra-high pressure, metamorphism.

Introduction

There are a number of high-pressure TiO$_2$ polymorphs having a higher density than rutile (space group $P4_2/mnm$). Static compression coupled with laser heating indicated the existence of a hexagonal-like structure of TiO$_2$, which may be related to the fluorite type and which reverts to the α-PbO$_2$ structure upon release of pressure (Liu, 1978). Later static compression studies at ambient temperature or up to 1527°C by laser heating showed the compression path rutile → α-PbO$_2$ type (space group $Pbcn$) → baddeleyite type (MI, space group $P2_1/c$) → orthorhombic OI structure (space group $Pbca$) → cotunnite type (OII, space group $Pnma$) (Sato et al., 1991; Dubrovinskaia et al., 2001; Dubrovinsky et al., 2001). Recently, Nd-YAG-laser pulse irradiation of Ti target under oxygen background gas for the combined effects of oxidation and very rapid radiant heating/cooling was used to synthesize α-PbO$_2$-type (Chen & Shen, 2002) and fluorite-like TiO$_2$ condensates partly transformed into baddeleyite-type structure (Chen & Shen, 2004). Spherical TiO$_2$ nanocondensates were found to transform martensitically into baddeleyite-type and then α-PbO$_2$-type structures with accompanied transformation twinning, shearing and shape change into ellipsoid upon electron irradiation. The

relatively large particles followed the same transformation path yet with alternative lattice correspondence and additional multiple deformation twinning of the baddeleyite type (Chen & Shen, 2004). The existence of a cubic fluorite-like TiO$_2$ was further supported by the most recent static compression coupled with laser heating at a pressure of 48 GPa and temperatures between 1900 and 2100 K (Mattesini et al., 2004).

α-PbO$_2$-type TiO$_2$ can be transformed directly from rutile and the phase transformation pressure is lower for nanophase material (~4 GPa and 900°C for the transformation of 10 nm-size particles) than for the bulk (~6 GPa and 850°C) (Olsen et al., 1999). This knowledge gives indicative P-T constraints on the natural occurrence of α-PbO$_2$-type TiO$_2$, recently identified by analytical electron microscopy as an epitaxial nanometer-thick slab between twinned rutile bicrystals included in almandine-rich garnet of diamondiferous quartzo-feldspathic rocks in the ultra-high pressure (UHP) metamorphic terrane of Saxonian Erzgebirge, Germany (Hwang et al., 2000). [UHP refers to metamorphic pressure above 2.5 to 2.7 GPa for the production of coesite (Liou et al., 1998).] The Saxonian Erzgebirge continental crustal rocks were therefore suggested to have been buried to a depth of at least 200–130 km (Hwang et al., 2000).

On the other hand, the so-called geniculated twin of rutile, without α-PbO$_2$-type TiO$_2$ slab at the twin boundary, was commonly found in crustal rocks (Deer *et al.*, 1992) and white schist from the Kulet region in the Kokchetav UHP massif, Kazakhstan as documented here. It is an open question whether these twinned rutile bicrystals were a result of phase transformation from the primary α-PbO$_2$-type TiO$_2$ at high pressure or due to a shear stress during exhumation in UHP terrane. Here we clarify by extraction (*i.e.* ion milling to remove matrix constraint) and electron irradiation that the decompression of α-PbO$_2$-type TiO$_2$ would cause more complicated transformation rather than twinned bicrystals of rutile. The observed cubic and amorphous pathways are interesting, comparing with the previous proposal of modified fluorite-type phase for dioxides (Haines & Léger, 1997; Chen & Shen, 2004). We suggest also, based on (hydrothermal) high T-P experiments and nanoparticle coalescence results (Tsai *et al.*, 2004), that such a geniculated twin of rutile without α-PbO$_2$-type TiO$_2$ relic was more likely formed by an alternative growth/coalescence process during metamorphism either in the presence of solution, or simply in the solid state.

Natural samples and experimental procedures

α-PbO$_2$-type TiO$_2$ occurs as an epitaxial nanometer-thick slab between twinned rutile bicrystals in almandine-rich garnet of diamondiferous quartzo-feldspathic rocks from the Saxonian Erzgebirge, Germany (Hwang *et al.,* 2000). The highest metamorphic P-T conditions of this UHP terrain have been estimated around 7.0 GPa and 1200°C and the age of the peak metamorphism, around 340 Ma (Massonne & O'Brien, 2003). On the other hand, the twinned rutile bicrystals without α-PbO$_2$-type TiO$_2$ occur as inclusions of garnet in white schist collected from the Kulet area, Kazakhstan, where diamondiferous UHP rocks of the Kokchetav massif outcrop (Sobolev & Shatsky, 1990). The peak metamorphic P-T conditions of this UHP terrain have been estimated around 5.8–6.5 GPa and 900–1100°C and the age of the peak metamorphism, around 530–540 Ma (Parkinson *et al.*, 2002).

Thin sections of quartzo-feldspathic rock and white schist from the above two localities were studied by optical microscopy under plane polarized light. Selected areas of garnet with inclusions were Ar-ion milled to electron transparency and then studied by analytical electron microscopy (AEM, JEOL 3010 at 300 keV for imaging and energy dispersive X-ray (EDX) analysis). Transmission electron microscopy and selected area electron diffraction (SAED) patterns were used to identify the titania inclusions in garnet. Lattice image and two-dimensional Fourier transform as well as reconstructed image were used to study the defects and phase transformation of the titania phases upon garnet host removal and electron irradiation under 300 keV and a beam current of 60 pA/cm^2.

The Al$_2$O$_3$–TiO$_2$ gel was selected as starting material of high P-T experiments, because it may mimic the chemical characteristics of a peraluminous metamorphic rock and enables studying the effect of Al dissolution on the phase change and defects formation, if any, of TiO$_2$. The (hydrothermal) high T-P experiments were carried out by first synthesizing a Al$_2$O$_3$–TiO$_2$ (78:22 in molar ratio or 82:18 in weight ratio) gel after the method of Montoya *et al.* (2001). In this sol-gel route, acid co-hydrolysis of precursors, *i.e.* aluminum tri-sec-butoxide Al(OBu^s)$_3$ (ATSB) and titanium(IV) tetrabutoxide Ti(OBu^n)$_4$(TTB), was conducted in isopropanol solvent. Aluminum and titanium alkoxides were dissolved in 300 ml of isopropanol at 25°C. The mixture was maintained under vigorous stirring for 3 hours, followed by the dropwise addition of water. Isopropanol and HNO$_3$ solution, with specific reactants, were used in order to obtain the following molar ratios: HNO$_3$/(ATSB+TTB) = 0.2; H$_2$O/(ATSB+TTB) = 20; ROH/(ATSB+TTB) = 75. Beyond the gelation point, the material was aged without agitation for 4 days, and heated in oven for 3 hours (at a final temperature of 85.5°C) to form wet gel with 18 wt % TiO$_2$ in solid solution.

Experiments were further performed in a piston cylinder apparatus at 675°C, 8.5 kbar or 800°C, 9 kbar for 72 h using a half-inch diameter chamber. The chosen P-T conditions fall into the range of amphibolite to granulite facies metamorphism. The furnace assembly was constructed from graphite, talc and pyrophyllite. The pulverized gel was sealed in gold capsules with or without 10 wt % addition of H$_2$O and then subjected to high T-P conditions. The temperatures, measured with chromel-alumel thermocouples, were accurate to $\pm$ 10°C. The hydraulic pressure was measured using a Heise gauge. All runs were brought to 200 MPa above the desired experimental pressure at room temperature. Then the pressure was adjusted to the experimental pressure after the temperature was raised to the experimental temperature. The reported pressure is nominal. The gel powder under high T-P and hydrothermal conditions was not sintered, *i.e.* remained as loose aggregate, and ready for phase identification by powder X-ray diffraction in the 2θ range of 10 ~ 70° using a D-5000 Siemens diffractometer with Cu $K\alpha$ radiation at 40 kV and 30 mA.

Results

Decompression of α-PbO$_2$-type TiO$_2$ slab sandwiched between rutile twins

The nanometer-thick α-PbO$_2$-type TiO$_2$ slab between twinned rutile bicrystals in almandine-rich garnet of diamondiferous quartzo-feldspathic rocks from the Saxonian Erzgebirge, Germany (Hwang *et al.,* 2000) (Fig. 1a) was Ar-ion milled to remove the matrix of garnet and part of the rutile (Fig. 1b) for further AEM study. The garnet host removal enabled accurate EDX composition determination (not shown) of TiO$_2$ inclusion, showing it to be free of impurities. Lattice image (Fig. 2a) indicated that the α-PbO$_2$-type TiO$_2$ slab with slight dosage of electrons was still under effective matrix constraint of the twinned rutile bicrystals yet with amorphous region at the sample edge. Two-dimensional Fourier transform and reconstructed image (Fig. 2b and 2c, respectively) showed dislocations with {1$\bar{1}$1} and {1$\bar{1}$0} half planes and (002) slip plane for the α-PbO$_2$-type TiO$_2$ slab.
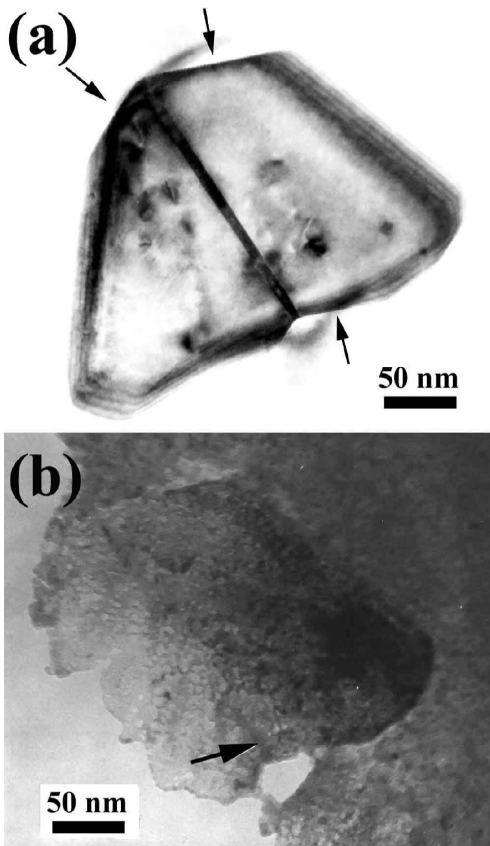
Fig. 1. TEM bright field image of (a) intact titania inclusion in garnet matrix showing α-PbO$_2$-type TiO$_2$ slab at the boundary of twinned bicrystals of rutile with {110} faces edge-on (arrows), after Hwang *et al.* (2000), (b) the same titania inclusion in (a) with garnet matrix and part of rutile bicrystals removed by Ar-ion milling. Note (b) is from the same butterfly-like titania after more than one year of dwelling at ambient condition followed by Ar-ion milling to remove the garnet matrix. Arrow indicates the original position of α-PbO$_2$-type TiO$_2$ slab.

Further electron irradiation for minutes triggered a martensitic-type transformation of the α-PbO$_2$-type TiO$_2$ slab into unexpected denser baddeleyite-type structure (monoclinic, yet indexed according to distorted version of the cubic-fluorite-type structure denoted as f) (Fig. 3). Electron irradiation at energy as high as 1.25 MeV, in order to have ballistic knock-on events in the electron beam, was shown to promote graphite to diamond transition (Lyutovich & Banhart, 1999). However, in the present case of electron irradiation with a much lower energy (300 keV) on a nanometer-scale structure in a twin plane/grain boundary, phase transformation may be established by other factors such as surface energy, as discussed later, and lattice strain as a result of restricted expansion of the α-PbO$_2$-type TiO$_2$ slab under the constraint of rutile with rather high isothermal bulk modulus (B$_o$=210 GPa; Olsen *et al.*, 1999). Two-dimensional Fourier transform and reconstructed image (Fig. 3b and 3c) showed dislocation with {001} half plane and (100) slip plane for this fluorite-type related phase. The epitaxial relationship [110]$_\alpha$//[010]$_f$; (002)$_\alpha$//(001)$_f$; ($\bar{1}$10)$_\alpha$//(100)$_f$ was determined based on Fig. 2 and 3.

The rutile bicrystals suffered drastic deformation upon relaxation/transformation of the embedded α-PbO$_2$-type TiO$_2$ slab as manifested by one of the twin variants (Fig. 4). Lattice image (Fig. 4a), two-dimensional Fourier transform (Fig. 4b) and reconstructed image (Fig. 4c) showed abundant dislocations with (1$\bar{1}$0) and (011) half planes for the rutile. The rutile was further deformed, possibly due to stress-build-up next to the decomposing α-PbO$_2$-type TiO$_2$ slab, to cause disordering as indicated by the absence of ($\bar{0}$11) and (101) diffractions in the two-dimensional Fourier transform (Fig. 5a) and mis-registry of atoms/clusters in the reconstructed image (Fig. 5b). The satellite diffractions of (202) and (112) in Fig. 5a can possibly be attributed to such mis-registered atoms/clusters analogous to defect clustering of paracrystals in other transition metal oxides (Li & Shen, 2004 and literature cited therein). SAED pattern indicated that the diffractions of α-PbO$_2$-type TiO$_2$ slab and the twin spots of rutile bicrystals (Fig. 6a) became dimmed and finally disappeared after prolonged electron irradiation. The absence of (011) and (101) diffractions in the SAED pattern for severely deformed rutile (Fig. 6b) is in accord with the two-dimensional Fourier transform of the local area of one of the twin variants in Fig. 5. The retained diffractions (1$\bar{1}$0), (112) and (202) suggest a new disordered structure as derived from the supergroup rutile ($P4_2/mnm$). The transformed rutile in fact suffered considerable bending stress as indicated by uneven diffraction contrast in the dark field image with sample foil tilted slightly from the [111] zone axis (Fig. 7a and 7b). The α-PbO$_2$-type TiO$_2$ slab became amorphous, after prolonged AEM observations, as indicated by lattice image and the two-dimensional Fourier transform (not shown).

Twinned rutile bicrystals in Kokchetav white schist

Twinned rutile bicrystals were found as submicron-size inclusion in garnet of white schist from the Kulet area, Kokchetav massif (Fig. 8). According to electron diffraction, there is no epitaxial crystallographic relationship between the twinned rutile bicrystals and the garnet host. This indicates that the titanium was incorporated by porphyroblastic growth of garnet rather than exsolution. [Rutile exsolution from garnet may occur due to solubility change with pressure (0.8–4.5 wt % TiO$_2$ between 5 and 15 GPa) as determined experimentally using the multianvil high-pressure apparatus (Zhang *et al.*, 2003). However, in such a case, epitaxial rather than nonepitaxial crystallographic relationship is required, in order to lower the activation energy for the nucleation of rutile from garnet. The epitaxial precipitation was typically manifested by rutile needles or rods distributed along three crystallographically oriented planes in garnets of Sulu UHP eclogite (*cf.* Fig. 2 of Zhang *et al.*, 2003). Thus, the nonepitaxial and rather localized rutile bicrystals inclusion in garnet of Kokchetav white schist cannot be reasonably attributed to an exsolution process, but could result from grain inclusion during garnet growth.] TEM bright field image (Fig. 8a) and corresponding SAED pattern (Fig. 8b) showed that the twinned rutile bicrystals have (011) twin boundary and {110} faces exactly the same as in Fig. 1, ex-
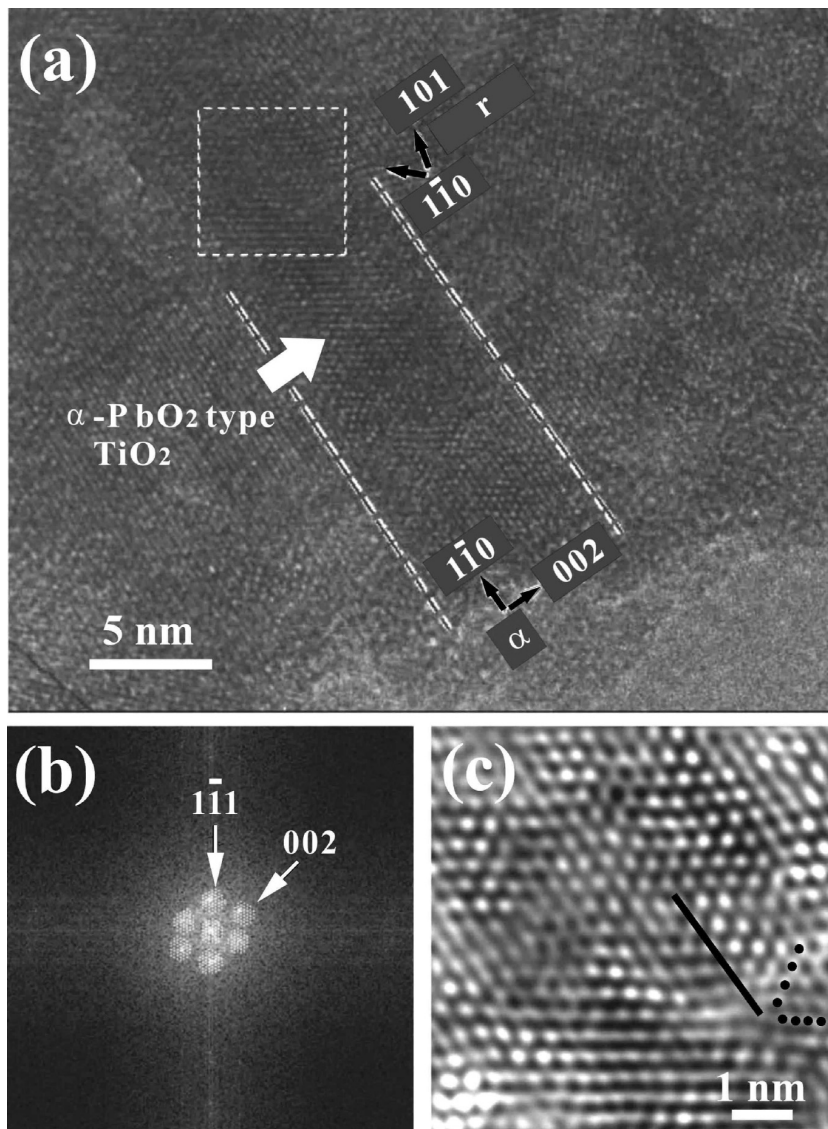
Fig. 2. (a) TEM (lattice image) of the α-PbO$_2$-type TiO$_2$ slab (α) still under effective constraint of the epitaxial rutile bicrystals (r) yet with amorphous region at the sample edge of Fig. 1b. (b) two-dimensional Fourier transform and (c) reconstructed image of the square region in (a) showing dislocations with $\{1\bar{1}1\}$ and $\{1\bar{1}0\}$ half planes (denoted as dotted lines) and (002) slip plane (denoted as solid line).

cept for the absence of α-PbO$_2$-type TiO$_2$ at the twin boundary. Having no evidence of exsolution from garnet and no α-PbO$_2$-type TiO$_2$ relic, it is not justified to assume a precursor phase of α-PbO$_2$-type structure for unusually deep burial for ultra-high pressure terranes as discussed later.

Static compression of TiO$_2$-Al$_2$O$_3$ gel

Optical microscopy under plane polarized light showed that a geniculated twin of rutile was crystallized from TiO$_2$-Al$_2$O$_3$ hydrous gel upon static compressions at 675°C and 8.5 kbar for 72 h (not shown) or 800°C and 9 kbar for 72 h (Fig. 9a). TEM bright field image and corresponding SAED pattern (Fig. 9b) showed that the twinned rutile bicrystals have (011) twin boundary exactly the same as in Fig. 8. The formation of twinned rutile bicrystals was not affected by the presence of additional water and alumina hydrate/alumina in the synthesis. SEM coupled with EDX analysis of the sample fired at 800°C and 9 kbar for 72 h (Fig. 10) indicated the twinned rutile contained some dissolved Al and was

about the same size as that synthesized at a slightly lower T-P conditions. The twinned rutile formed in the present sol-gel route is two orders of magnitude larger in size than the natural bicrystals in white schist (Fig. 8). This indicates that the submicron-size twinned rutile inclusion in garnet of the white schist could be formed by solid-state or fluid-assistant metamorphic processes before being isolated from the source material by the garnet host.

Discussion

Relaxation/transformation of α-PbO$_2$-type TiO$_2$

The nanometer-thick α-PbO$_2$-type TiO$_2$ slab at the twin boundary of rutile bicrystals has a considerable residual stress. Given the refined cell parameters ($a = 0.459$ nm, $b = 0.544$ nm, $c = 0.494$ nm) (Hwang *et al.*, 2000) and reported parameters (Olsen *et al.*, 1999) of the Birch-Murnaghan equation of state, *i.e.* isothermal bulk modulus $K_T = 258$ GPa, K' = 4.05 and zero-pressure molar volume $V_o =$
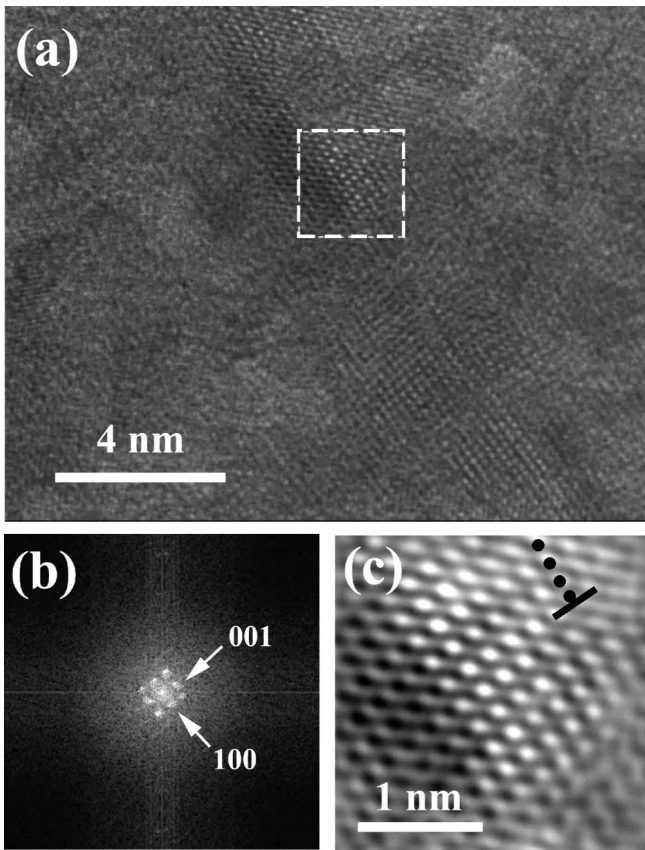
Fig. 3. (a) TEM (lattice image) of the α-PbO$_2$-type TiO$_2$ slab of Fig. 2a subject to electron irradiation for minutes to transform into baddeleyite-type structure (indexed according to distorted version of the cubic-fluorite-type structure) due to the restricted expansion of the slab under the constraint of rutile with rather high bulk modulus (see text). (b) two-dimensional Fourier transform and (c) reconstructed image of the square region in (a) showing dislocation with {001} half plane (denoted as dotted line) and (100) slip plane (denoted as solid line). Note the epitaxial relationship $[110]_\alpha//[010]_f$; $(002)_\alpha//(001)_f$; $(\bar{1}10)_\alpha//(100)_f$ is slightly different from the dense titania condensates fabricated by laser ablation technique (Chen & Shen, 2004) (*cf.* text).

0.1219 nm^3, a residual stress of 1.47 GPa was then calculated for α-PbO$_2$-type TiO$_2$. The garnet and rutile has a rather high isothermal bulk modulus of K$_T$ = 165 GPa (Verma, 1960) and 210 GPa (Olsen *et al.*, 1999), respectively, to exert effective volume constraint during decompression to prevent α-PbO$_2$-type TiO$_2$ from back-transformation to rutile (Hwang *et al.*, 2000). Upon electron irradiation and/or removal of garnet/rutile host, the α-PbO$_2$-type lattice was significantly expanded, distorted and subsequently became amorphous with accompanying shearing of the adjoined rutile bicrystals to form dislocations and faults.

The relaxation/transformation bifurcation of α-PbO$_2$-type TiO$_2$ can be rationalized by the combined effects of electron irradiation and volume constraint removal. Atoms can possibly be displaced by ballistic knock-on events in the electron beam at very high energy (Lyutovich & Banhart, 1999) as mentioned. For the nanometer-thick α-PbO$_2$-type TiO$_2$ slab at the twin boundary of rutile bicrystals, it is a rather complicated yet effective compressive and shear stress that caused the shuffling of the lattice into fluorite- or baddeleyite-like unit more vulnerable to electron dosage. Shear stress has been proven by diamond anvil cell (Wu *et al.*, 1993) and ball milling (Begin-Colin *et al.*, 1994) to promote polymorphic high-pressure transformation of olivine and TiO$_2$, respectively. The dislocation geometry suggests significant shearing along {100}$_f$ and (001)$_\alpha$, the same as the nano-size baddeleyite-type TiO$_2$ condensates which were fabricated by laser ablation technique and back-transformed martensitically into α-PbO$_2$ type TiO$_2$ upon electron irradiation (Chen & Shen, 2004). The present epitaxial relationship $(001)_\alpha//(001)_f$; $\{110\}_\alpha//\{100\}_f$, however, turns out to be different from $(001)_\alpha//(001)_f$; $(110)_\alpha//(110)_f$ and $(100)_\alpha//(010)_f$; $(02\bar{1})_\alpha//(100)_f$ as determined for the nano-size and much larger titania condensates, respectively (Chen & Shen, 2004). [The relatively large particles also transformed upon electron irradiation into baddeleyite type and then partially into α-PbO$_2$ type yet with a lattice correspondence $[010]_f//[100]_\alpha$; $(100)_f//(02\bar{1})_\alpha$ different from that of nano-sized particles, and are complicated by primary and secondary deformation twin variants of the baddeleyite type following {100} and {110} twin planes (*cf.* Fig. 5 of Chen & Shen, 2004).] The discrepancy may be attributable to specific resolved shear stress under the influence of lateral constraint for the slab, and the nano-size/coherency strain effect in the free condensates (Chen & Shen, 2004). It is also possible that very rapid cooling rate of small TiO$_2$ condensates (*e.g.* 1 x 10^9 K/s for diameter = 10 nm (*cf.* Appendix of Chen & Shen, 2002) under laser and background gas caused unique crystallographic relationship for specific condensate size (Chen & Shen, 2004). Temperature may play an important role on the synthesis of fluorite-like TiO$_2$ using laser ablation condensation (Chen & Shen, 2004) or a laser-heated diamond anvil cell (Mattesini *et al.*, 2004). Competition between the pathways, in particular the cubic post-rutile phases with $Pa\bar{3}$ and fluorite structures for dioxides (Haines & Léger, 1997), might explain the observed amorphization on decompression. Surface energy may also be of concern in the amorphization of nano-sized crystalline phase. In this regard, size-dependent enthalpy measurement of dioxides (*e.g.* zirconia) by oxide melt solution calorimetry indicated that the amorphous material has a lower surface energy than crystalline polymorphs (*i.e.* tetragonal and monoclinic symmetry as derived from cubic fluorite-type structure) (Navrotsky, 2003).

In any case, the present shuffling scheme is analogous to the opposite transformation from fluorite- or baddeleyite-like TiO$_2$ condensates into α-PbO$_2$-type structure upon electron irradiation (Chen & Shen, 2004), both being in accord with topological distortion of three-dimensional anion nets of a parent cubic fluorite structure (Hyde *et al.*, 1972). [The proposed sequence of pressure-induced phase transitions in rutile-structured metal dioxides (*e.g.* SnO$_2$, PbO$_2$ and RuO$_2$), which serve as models for the behavior of stishovite at high pressures, has been quite a debate. In particular it centers around topological distortions of three-dimensional anion nets (Hyde *et al.*, 1972) to form cubic high-pressure phase of fluorite structure (space group *Fm3m*) with an increase in cation coordination number from 6 to 8 (Haines &
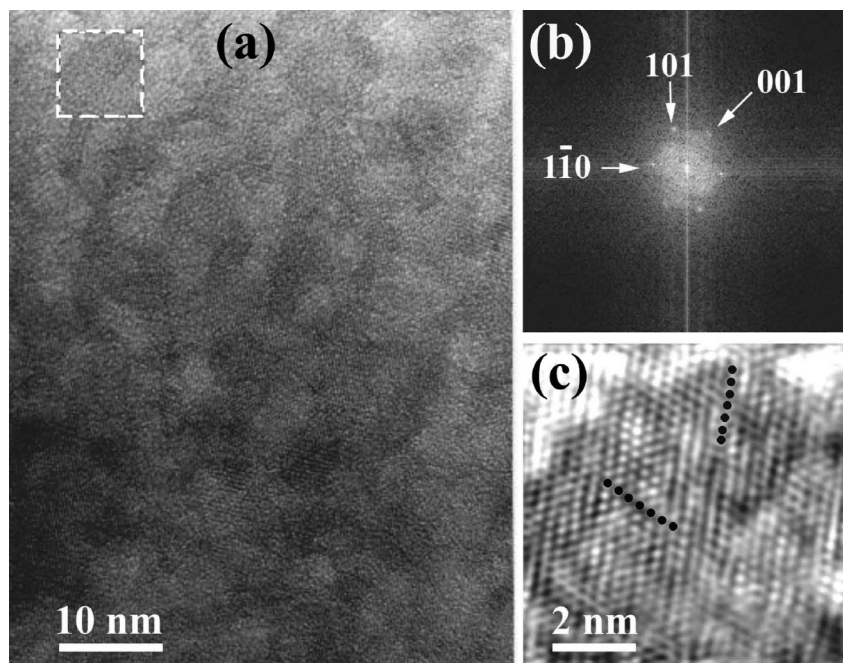
Fig. 4. (a) TEM (lattice image) of one of the rutile bicrystals in Fig. 3a significantly deformed due to the relaxation/transformation of the α-PbO$_2$-type TiO$_2$ slab. (b) two-dimensional Fourier transform and (c) reconstructed image of the square region in (a) showing dislocations with (1$\bar{1}$0) and (011) half planes (denoted as dotted lines).
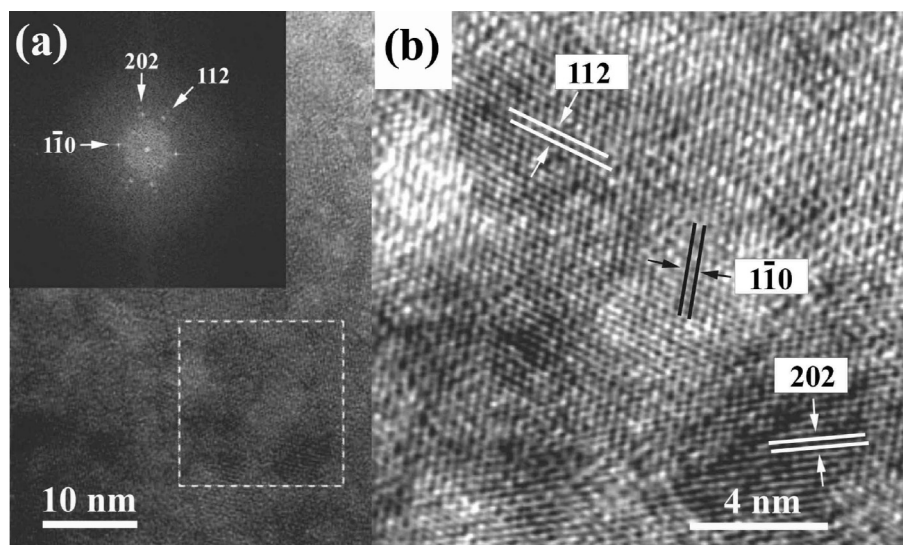

Fig. 5. (a) TEM (lattice image) of one of the rutile bicrystals in Fig. 4a further deformed due to the stress build-up next to the decomposing α-PbO$_2$-type TiO$_2$ slab. The inset two-dimensional Fourier transform and (b) reconstructed image of the square region in (a) indicated that (011) and (101) diffractions of rutile were disappeared, whereas (1$\bar{1}$0) of rutile retained. Such a disordering caused misregistry of atoms/clusters in the reconstructed image.

Léger, 1993), or alternatively, *Pa*3 modified fluorite-type structure with 6 short and 2 long polyhedral cation-oxygen distance (Haines *et al.*, 1996; Haines & Léger, 1997).] The martensitic-type transition process observed here took place under a considerable heating effect by electron irradiation and a residual stress of 1.47 GPa as mentioned. Regardless of the stress level and undercooling at departure from equilibrium phase boundary, the martensitic-type transformation did not create the twinned bicrystals shaped in mirror image. Deformation by an applied force such as ball milling (Begin-Colin *et al.*, 1994) or in natural process as manifested by Dabie UHP jadeite-quartzite containing rutile with polysynthetic {011} twin domains (Meng *et al.*, 2004) would cause multiple twinning and stacking faults rather than bicrystals with a single twin plane. [According to Begin-Colin *et al.* (1994), the high-pressure modification of TiO$_2$ with an α-PbO$_2$-type structure

was formed transiently during room-temperature grinding of anatase. Rutile is the only phase present after prolonged ball milling.] On the other hand, hydrothermal experiments of sol-gel TiO$_2$-Al$_2$O$_3$ performed in the piston-cylinder apparatus at 675°C, 8.5 kbar up to 800°C, 9 kbar produced twinned bicrystals shaped in mirror image as the case in Kokchetav white schist.

Note that the present relaxation/transformation of α-PbO$_2$-type TiO$_2$ was conducted by electron beam heating under a residual stress of 1.47 GPa. At higher temperatures and lower rates of decompression, α-PbO$_2$-type TiO$_2$ may transform completely into equilibrium rutile with twin variants analogous to the coarsening of metastable α-PbO$_2$-type TiO$_2$ precipitates formed in sapphire under the combined effects of Al-impurity and matrix constraint (Xiao *et al.*, 1997). [According to Xiao *et al.* (1997), the first phase to precipitate in Ti-doped
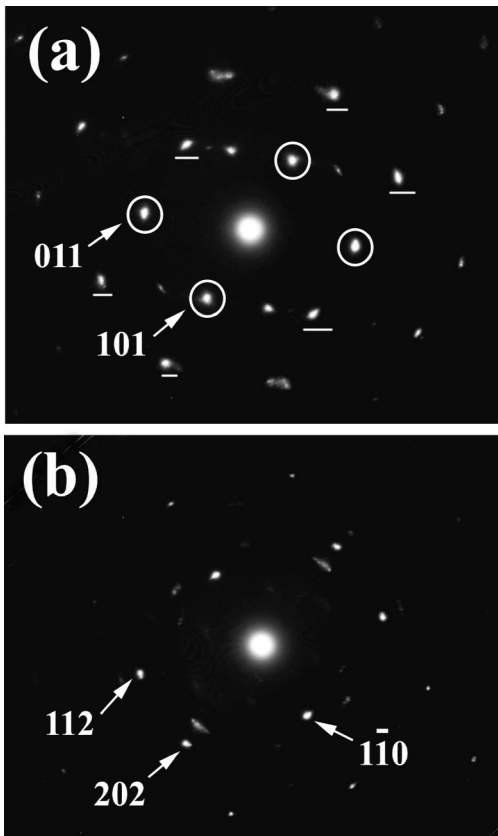
Fig. 6. Selected area electron diffraction (SAED) pattern of (a) the α-PbO₂-type TiO₂ slab and the twinned rutile bicrystals with garnet matrix completely removed. (b) SAED pattern taken after electron irradiation for ten minutes with resultant absence of (011) and (101) diffractions of rutile (denoted by circles in (a)) as well as twin spots of rutile and the diffractions of the α-PbO₂-type TiO₂. The ($1\bar{1}0$), (112) and (202) (underlined in (a) and labeled in (b)) were retained to form a new disordered structure from rutile ($P4_2/mnm$).
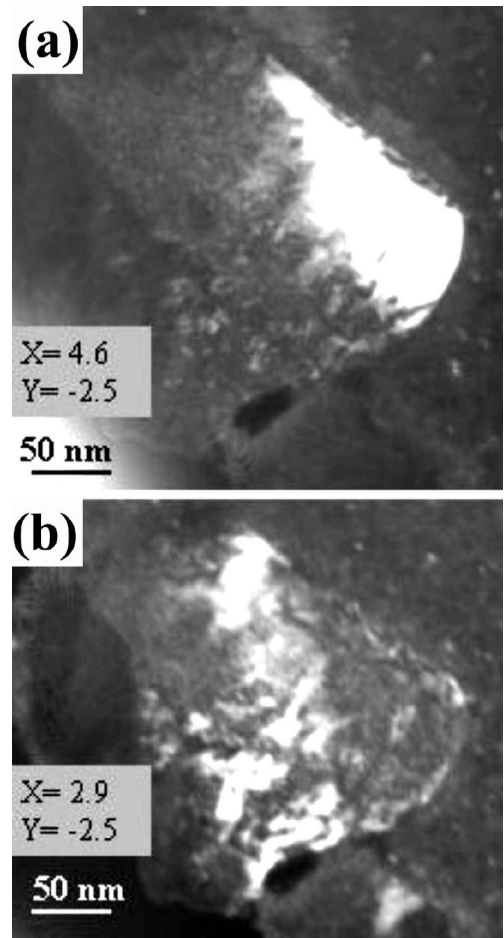

Fig. 7. (a) and (b) TEM (dark field image $g = 011$) with specified X/Y double tilting angles (degree) from [111] zone axis showing the transformed rutile variant has suffered considerable bending stress to give uneven diffraction contrast.

(moderate Ti level 500–1000 ppm) sapphire (Ti:α-Al₂O₃) single crystals annealed at 1300°C in air is a high-pressure form of TiO₂ with the α-PbO₂ structure. The coarsened disk-like α-PbO₂-type TiO₂ was found to transform into twinned rutile variants upon annealing at 1300°C for 30 h. Although the transformation from α-PbO₂-type TiO₂ to rutile is purely structural, its rate is controlled by atomic diffusion; the increased atomic volume of rutile compared with α-PbO₂-type TiO₂ is accommodated by expelling the extra mass of Al₂O₃ into nearby interstitial dislocation loops and is associated with a change in the precipitate morphology.] Still, twinned rutile bicrystals should not be taken as evidence of back-transformation from α-PbO₂-type TiO₂, as they can readily crystallize in amphibolite to granulite facies or even in eclogite facies metamorphism as mentioned above and discussed below.

Growth/coalescence as twinning mechanism of rutile bicrystals

One would expect a twinned bicrystals to nucleate at the twin plane, with negligible lattice strain at the twin bound-

ary. If the presence of the high-pressure phase is an indicator of post-rutile pressures, either the crystal must have first grown as a rutile twin and then transformed to α-PbO₂-type TiO₂, or the rutile 'twins' have formed around the α-PbO₂-type TiO₂, with the twin orientations being prescribed by the α-PbO₂-type TiO₂ lattice. The latter is rather unlikely since there is only one single shearing plane, *i.e.* (001), for the back transformation of α-PbO₂-type TiO₂ (Hyde & Andersson, 1989). Under such a case, both shearing along [010] and [0$\bar{1}$0] would occur in order to relieve matrix constraint and the resultant rutile would be full of polysynthetic nanotwins on (011) rather than forming bicrystals shaped in minor image. A pro-grade process, for the formation of the twinned bicrystals of rutile and then α-PbO₂-TiO₂ at the twin boundary, is also against an exsolution event for the titania inclusions in garnet of diamondiferous quartzo-feldspathic rocks from the Saxonian Erzgebirge, Germany (Hwang *et al.*, 2000).

Twinned bicrystals of rutile are common in crustal metamorphic rock (Deer *et al.*, 1992), and proven being able to crystallize from gels by the present hydrothermal/solid-state high-temperature and high-pressure experiments. Without supporting evidence of transformation twinning and deformation twinning (Buerger, 1945) for the inclusions in garnet
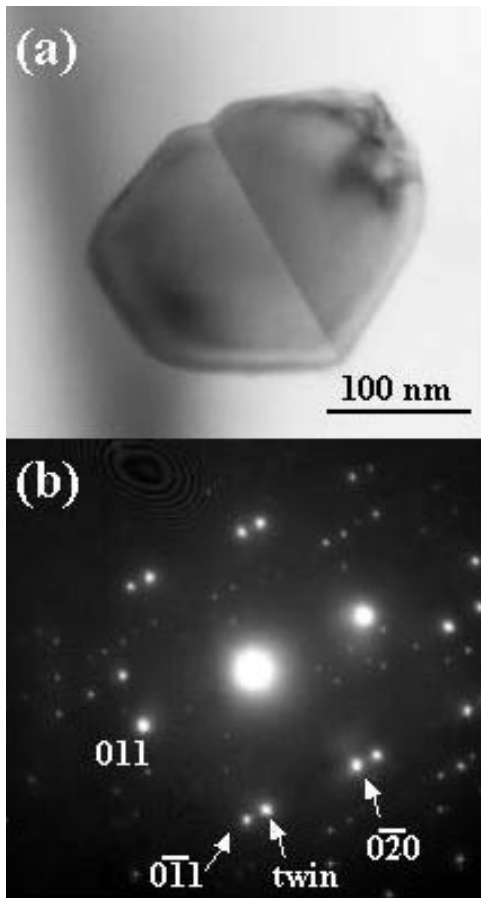
Fig. 8. (a) TEM (bright field image) of twinned rutile bicrystals, as inclusion in garnet of the white schist from the Kulet region, Kokchetav massif, with (011) twin boundary edge-on and {110} faces inclined to electron beam direction, and (b) corresponding SAED pattern in [100] zone axis showing twin spots of rutile, garnet matrix and double diffractions.

of white schist, we suggest alternatively that the geniculate twinning of rutile is due to a growth/coalescence event. Growth twins are commonly equal in size and may even have bicrystals shaped in mirror image, as the twinned rutile in the Kokchetav white schist. Twin boundary may facilitate growth either in a solid-state or fluid-involved crystallization process. On the other hand, coalescence twinning was originally suggested for (111)-specifically impinged fluorite-type oxides with opposite fcc stacking sequence (Lee & Shen, 1999). Recently, rutile nanoparticles prepared by laser ablation on Ti target were found to have well-developed {110} and {011} surfaces with steps for {~110} and {~011} vicinal attachment, causing respectively edge dislocations and planar defects, *i.e.* fault and twin for rutile crystal. The {011}-interface relaxation, by shearing along <011> directions, accounts for a rather high density of edge dislocations near the planar defects thus formed. Brownian motion, even valid in solid state (Kuo & Shen, 1997; Chen & Shen, 1997), may proceed above a critical temperature for anchorage release at the interface of imperfect attached nanoparticles until an epitaxial relationship is reached.

Phase boundary of rutile and α-PbO$_2$-type TiO$_2$ and implications for natural occurrence

In situ high-pressure and high-temperature studies (Olsen *et al.*, 1999) employing the multi-anvil device and white-beam (using synchrotron radiation source) energy-dispersive method indicated that the transformation pressure is lower for nano-phase material (10 nm at ~4 GPa and 900°C) than for the bulk (0.7 μm at ~6 GPa and 850°C). It should be noted that phase change of a nanometer-scale structure in a twin plane/grain boundary may be established by other forces. Even for bulk nanoparticles, the surface energy may stabilize a phase under conditions where the macro-phase would not be stable (*e.g.* Navrotsky, 2003). And in a grain boundary, where lattice strain comes into play, the situation is even more complex. In short, equilibrium thermodynamics for a
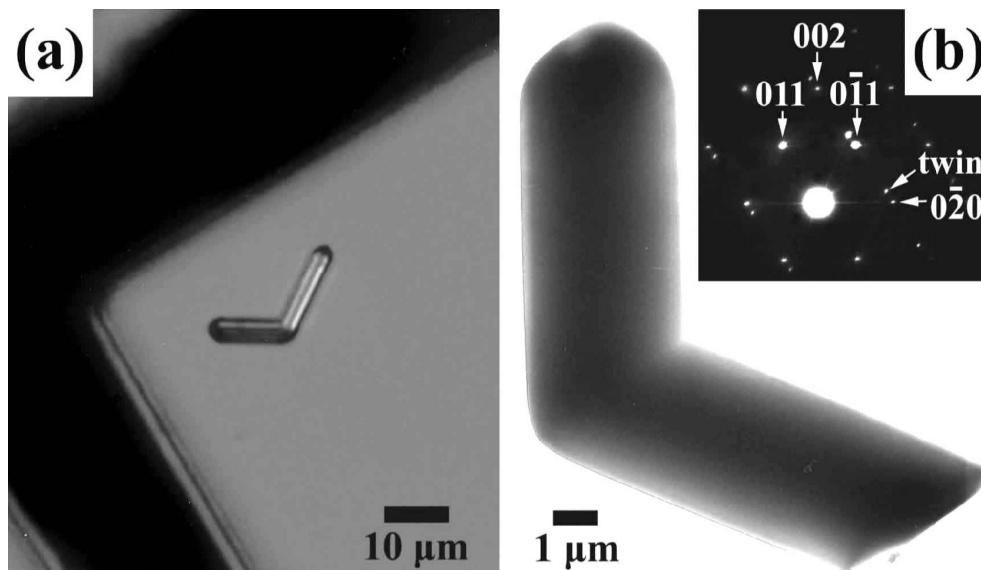

Fig. 9. (a) Optical micrograph under plane polarized light (crossed polarizers) of synthetic sample showing geniculated twinning of birefringent rutile with the horizontal one in parallel extinction as indicated by the red color of inserted λ plate. (b) TEM bright field image and corresponding SAED pattern inset in [100] zone axis showing the twinned rutile bicrystals have (011) twin boundary.
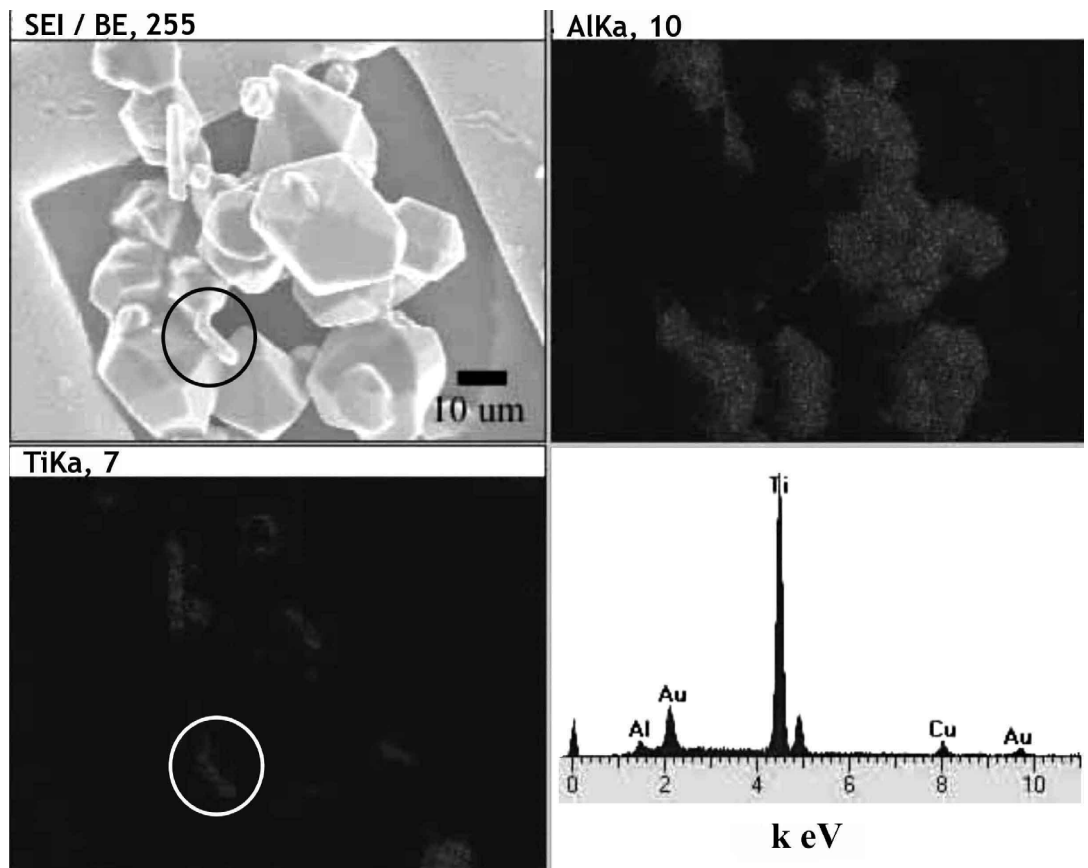
Fig. 10. Scanning electron micrograph and X-ray mappings of geniculate-twinned rutile (indicated by circle) and corundum crystallized from TiO_2-Al_2O_3 hydrous gel at 800°C and 9.0 kbar for 72 h in the presence of additional water. Point-count EDX spectrum indicates that the rutile crystals are slightly dissolved with Al.

macro-phase are unlikely to apply to grain boundary of nano-phases. Hydrothermal phase equilibrium experiments performed in the multi-anvil apparatus bracket the phase boundary at 700, 1000, and 1200°C, indicating that the equilibrium phase boundary can be described by the equation: P (GPa) = 1.29 + 0.0065 T (°C) unaffected by the presence of water (Withers *et al.*, 2003).

The rutile bicrystal inclusions in garnet of Kulet whiteschist contain no α-PbO₂-type-TiO₂ and have nothing to do with an exsolution process, as mentioned above. Therefore there is no evidence to claim a primary high-pressure phase as the precursor of these inclusions. Aside from the controversy of kinetics phase boundary, the absence of α-PbO₂-type TiO₂ indicated that twinned rutile bicrystals in white schist of Kokchetav massif in this study were subject to a burial depth no more than that required to form diamond. In fact, the phase diagram of either Akaogi *et al.* (1992) or Withers *et al.* (2003) suggests that the natural occurrence of α-PbO₂-type TiO₂ requires formation pressures considerably higher than the graphite-diamond phase boundary (Withers *et al.*, 2003).

Concluding remarks

With effective matrix constraint, the α-PbO₂-type TiO₂ was shown to transform into a fluorite-like unit and then decompose as an amorphous phase rather than forming twinned bicrystals. The observed relaxation process, although shedding light on the transformation pathways for dioxides in

general, does not necessarily exclude other transformation paths in nature. In essence, caution is required to employ the phase boundary of rutile and α-PbO₂-type TiO₂ as a thermobarometer following the phase diagram of Akaogi *et al.* (1992) or the recent hydrothermal equilibrium version of Withers *et al.* (2003). Since twinned bicrystals can be rationalized by a growth and/or coalescence process, it is not justified to assume a precursor phase of α-PbO₂-type structure for twinned rutile bicrystals if such a dense phase did not survive as relic. Rutile, unless exsolved epitaxially from a host mineral such as garnet, does not constitute evidence for unusually deep burial for ultrahigh pressure terranes.

References

Akaogi, M., Kusaba, K., Susaki, J.I., Yagi, T., Matsui, M., Kikegawa, T., Yusa, H., Ito, E. (1992): High-pressure high-temperature stability of α-PbO₂-type TiO₂ and MgSiO₃ majorite: calorimetric and *in*

situ X-ray diffraction studies. *in* "High-Pressure Research: Application to Earth and Planetary Sciences", Y. Syono & M.H. Manghnani, eds., TERRAPUB/Am. Geophys. Union, 447-455.

Begin-Colin, S., Le Caer, G., Mocellin, A., Zandona, M. (1994): Polymorphic transformations of titania induced by ball-milling. *Phil. Mag. Lett.*, **69**, 1-7.

Buerger, M.J. (1945): The genesis of twin crystals. *Am. Mineral.*, **30,** 469-482.

Chen, J. & Shen, P. (1997): On the rotation of nonepitaxy $Ni_{1-x}O$ particles within zirconia grain. *Scripta Materialia*, **37,** 1287-1294.

Chen, S.Y. & Shen, P. (2002): Laser ablation condensation of α-PbO2-type TiO_2. *Phys. Rev. Lett.*, **89**, 096106-1-4.

–,– (2004): Laser ablation condensation and transformation of baddeleyite-type related TiO_2. *Jap. J. Appl. Phys.*, **43,** 1519-1524.

Deer, W.A., Howie, R.A., Zussman, J. (1992): An Introduction to the Rock-Forming Minerals. Longman Scientific and Technical, Essex, 1-696.

Dubrovinskaia, N.A., Dubrovinsky, L.S., Ahuja, R., Prokopenko, V.B., Dmitriev, V., Weber, H.P., Osorio-Guillen, J.M., Johansson, B. (2001): Experimental and theoretical identification of a new high-pressure TiO_2 polymorph. *Phys. Rev. Lett.*, **87**, 275501-1-4.

Dubrovinsky, L.S., Dubrovinskaia, N.A., Swamy, V., Musca, J., Harrison, N.M., Ahuja, R., Holm, B., Johansson, B. (2001): The hardest known oxide. *Nature*, **410**, 653-654.

Haines, J. & Léger, J.M. (1993): Phase transitions in ruthenium dioxide up to 40 GPa: Mechanism for the rutile-to-fluorite phase transformation and a model for the high-pressure behavior of stishovite SiO_2. *Phys. Rev. B.*, **48**, 13344-13350.

–,– (1997): X-ray diffraction study of the phase transitions and structural evolution of tin dioxide at high pressure: Relationships between structure types and implications for other rutile-type dioxides. *Phys. Rev. B.*, **55**, 11144-11154.

Haines, J., Léger, J.M., Schulte, O. (1996): $Pa\overline{3}$ modified fluorite-type structures in metal dioxides at high pressure. *Science*, **271**, 629-631.

Hwang, S.L., Shen, P., Chu, H.T., Yui, T.F. (2000): Nanometer-size α-PbO2-type TiO_2 in garnet: A thermobarometer for ultrahigh-pressure metamorphism. *Science*, **288**, 321-324.

Hyde, B.G. & Andersson, S. (1989): Inorganic Crystal Structures. John Wiley & Sons, New York, 69-72.

Hyde, B.G., Bursill, L.A., O'Keeffe, M., Andersson, S. (1972): Continuous topological variation of coordination in crystals: Structural relations and possible transformation mechanisms. *Nature (London) Physical Science*, **237**, 35-38.

Kuo, L.Y. & Shen, P. (1997): On the rotation of nonepitaxy crystallites on single crystal substrate. *Surf. Sci.*, **373**, L350-L356.

Lee, W.S. & Shen, P. (1999): On the coalescence and twinning of cubo-octahedral CeO_2 condensates. *J. Cryst. Growth*, **205**, 169-176.

Li, M.Y. & Shen, P. (2004): On the nucleation and paracrystal interspacing of Zr-doped $Co_{3-\delta}O_4$. *Mater. Sci. Eng. B*, **111**, 82-89.

Liou, J.G., Zhang, R.Y., Ernst, W.G., Rumble III, D., Maruyama, S. (1998): High-pressure minerals from deeply subducted metamorphic rocks. *Rev. Mineral.*, **37**, 33-96.

Liu, L.G. (1978): A fluorite isotype of SnO_2 and a new modification of TiO_2: Implications for the Earth's lower mantle. *Science*, **199**, 422-425.

Lyutovich, Y. & Banhart F. (1999): Low-pressure transformation of graphite to diamond under irradiation. *Appl. Phys. Lett.*, **74**, 659-660.

Massonne, H.J. & O'Brien, P.J. (2003): The Bohemian Massif and the NW Himalaya. *in* "Ultrahigh Pressure Metamorphism", D.A. Carswell & R. Compagnoni, eds., Eotvos University Press, Budapest, 145-187.

Mattesini, M., de Almeida, J.S., Dubrovinsky, L., Dubrovinskaia, N., Johansson, B., Ahuja, R. (2004): High-pressure and high-temperature synthesis of the cubic TiO_2 polymorph. *Phys. Rev. B*, **70**, 212101-1-4.

Meng, D.W., Wu, X.L., Meng, X., Han, Y.J., Li, D.X. (2004): Domain structures in rutile in ultrahigh-pressure metamorphic rocks from Dabie Mountains, China. *Micron*, **35**, 441-445.

Montoya, J.A., Angel, P.D., Viveros, T. (2001): The effect of temperature on the structural and textural evolution of sol-gel Al_2O_3 – TiO_2 mixed oxides. *J. Mater. Chem.*, **11**, 944-950.

Navrotsky, A. (2003): Energetics of nanoparticle oxides: interplay between surface energy and polymorphism. *Geochem. Trans.*, **4**(6), 34-37. doi 10.1039/b308711e.

Olsen, J.S., Gerward, L., Jiang, J.Z. (1999): On the rutile/α-PbO$_2$-type phase boundary of TiO_2. *J. Phys. Chem. Solids*, **60**, 229-233.

Parkinson, C.D., Maruyama, S., Liou, J.G., Kohn, M.J. (2002): Probable prevalence of coesite-stable metamorphism in collisional orogens and a reinterpretation of Barrovian metamorphism. *in* "The Diamond-Bearing Kokchetav Massif, Kazakhstan", C.D. Parkinson, I. Katayama, J.G. Liou, S. Maruyama, eds., Universal Academy Press, Inc., Tokyo, 447-461.

Sato, H., Endo S., Sugiyama, M., Kikegawa, T., Shimomura, O., Kusaba, K. (1991): Baddeleyite-type high-pressure phase of TiO_2. *Science*, **25**, 786-788.

Sobolev, N.V. & Shatsky, V.S. (1990): Diamond inclusions in garnets from metamorphic rocks. *Nature*, **343**, 742-746.

Tsai, M.H., Chen, S.Y., Shen, P. (2004): Imperfect oriented attachment: accretion and defect generation of nanosize rutile condensates. *Nano Letters*, **4**[7], 1179-1201.

Verma, R.K. (1960): Elasticity of some high-density crystals. *J. Geophys. Res.*, **65**, 757-766.

Withers, A.C., Essene, E.J., Zhang, Y. (2003): Rutile/TiO_2 II phase equilibria. *Contrib. Mineral. Petrol.*, **145**, 199-204.

Wu, T.C., Bassett, W.A., Burnley, P.C., Weathers, M.S. (1993): Shear-promoted phase transitions in Fe_2SiO_4 and Mg_2SiO_4 and the mechanism of deep earthquakes. *J. Geophys. Res.*, **98**(B11), 19767-19776.

Xiao, S.Q., Dahmen, U., Heuer, A.H. (1997): Phase transformation of TiO_2 precipitates in sapphire induced by the loss of coherency. *Phil. Mag.*, **A75**, 221-238.

Zhang, R.Y., Zhai, S.M., Fei, Y.W., Liou, J.G. (2003): Titanium solubility in coexisting garnet and clinopyroxene at very high pressure: the significance of exsolved rutile in garnet. *Earth Planet. Sci. Lett.*, **216**, 591-601.